Low-frequency suppression of random-telegraph-noise spectra in high-temperature superconductors

V. D. Ashkenazy
Department of Physics, Bar-Ilan University, 52100, Ramat Gan, Israel

G. Jung
Department of Physics, Ben Gurion University of the Negev, 84105 Beer-Sheva, Israel and Instytut Fizuki, Polish Academy of Sciences, 02668 Warszawa, Poland

I. B. Khalfin
Department of Physics, Bar-Ilan University, 52100, Ramat Gan, Israel

B. Ya. Shapiro
Jack and Pearl Resnik Institute of Advanced Technology, Bar-Ilan University, 52100, Ramat Gan, Israel and Department of Physics, Bar-Ilan University, 52100, Ramat Gan, Israel

(Received 20 December 1993; revised manuscript received 29 July 1994)

Interaction of the random-telegraph-noise signals with pinned Abrikosov vortices in granular high-temperature superconductors is investigated. It is shown that the low-frequency part of random-noise spectra is suppressed due to interaction of Abrikosov vortices with pinning centers at low magnetic fields and/or due to mutual interactions of vortices in an Abrikosov lattice at high magnetic fields. Values of characteristic frequencies below which spectra are suppressed are evaluated for various experimental configurations including a typical experimental thin-film strip geometry. It is shown that characteristic frequencies and the functional dependence of the low-frequency part of the noise spectra strongly depend on the external magnetic field.

I. INTRODUCTION

High-T_c superconductors (HTSC) are characterized by strong manifestations of low-frequency noise in the form of $1/f$ fluctuations and pronounced random-telegraph-noise (RTN) signals.[1-8] For recent reviews, see Ref. 1 for flux noise and Ref. 2 for voltage noise. Although the detailed physical mechanism responsible for these fluctuations is still not fully known, it is generally recognized that a high level of low-frequency noise in HTSC materials is due to the high temperature of operation, strong anisotropy, and low pinning energies, resulting in relatively easy movements of flux vortices. Flux noise converts into voltage noise observed in thin HTSC films biased with the current flow exceeding the critical current of the sample.

$1/f$ flicker noise in solid-state systems is claimed to result from an incoherent superposition of many RTN signals generated by microscopic elementary two-level fluctuator (TLF's) possessing proper distribution of cutoff frequencies of their Lorentzian spectra.[9-13] This mechanism was confirmed by several experiments performed with submicron size samples containing only few, or even just a single TLF.[10,11,13] However, in high-T_c materials, along with $1/f$ noise and elementary fluctuators, we deal with yet another type of random-telegraph-noise signal. This particular RTN manifests itself in large samples, not of submicron dimensions, and is therefore claimed to be generated by the macroscopic two-level fluctuator (MTLF).[6] The characteristic feature of macroscopic RTN in HTSC is strong dependence of its power spectra on bias current, applied magnetic field, and temperature, as well as its appearance only within the limited "noisy window" range of bias parameters.[6-8] The duty cycle of the macroscopic RTN, defined as the ratio of the average lifetime of the system in the high-voltage state ("up" state) to the sum of average lifetimes in the low-voltage state ("down" state) and in the high-voltage states of the RTN, strongly depends on bias conditions and temperature.[5-8] The most pronounced macroscopic RTN were detected in granular HTSC films where extremely fast switching rates may extend the measurable noise spectra far into MHz frequencies.[8]

The shape of RTN Lorentzian power spectrum is fully determined by the amplitude of the signal, i.e., by the difference between the high and low signal levels, by the average lifetimes in both voltage levels, and by the background noise.[13] In particular the cutoff frequency of a RTN Lorentzian spectrum is determined by the sum of inverse of lifetimes in both levels. Usually, a symmetric RTN shows out close to the center of the noisy window and any deviation of the bias current and/or the magnetic field from the center of the noisy window causes the RTN to become asymmetric.[6]

The origin of macroscopic RTN in oriented or epitaxial HTSC films is most likely associated with random, activated changes in number of vortices participating in flux-flow or flux-creep dissipation processes. In granular films the generation of macroscopic RTN involves possibly two mechanisms: the fluctuator mechanism, responsible for activated random jumps of flux lines, and the detector action that couples flux noise to the observable voltages. There is strong experimental evidence that

direct conversion by intrinsic quantum interferometers constitutes the detector mechanism in granular HTSC films.[5] Another intriguing possibility is an integrated fluctuator-detector action predicted for serial-parallel arrangement of Josephson junction constituting intrinsic interferometer loops.[14,15]

Regardless of the mechanism laying behind the fluctuations, the RTN signal always causes random currents to flow in the HTSC sample. The random currents cause random Lorentz forces to act on vortices created inside the sample, either by the external magnetic field or by the self-field of the dc bias current. Moreover, in granular samples Lorentz force, apart from the random component in time, will possess a random component in space. Space randomness is due to the distribution of current density in the sample and to the distribution of magnetic induction in the grains.

Motion of vortices, caused by the interaction with random components of the Lorentz force, generates additional voltage across the sample that changes the power spectrum of RTN signal. The vortex-vortex interaction in the pinned Abrikosov lattice and/or interaction of vortices with bulk and surface pinning sites, opposes random force. As a result the power spectrum of the RTN signal will be suppressed at low frequencies. The extent and the frequency boundaries of this effect should depend on the elastic properties of the vortex lattice and on the structure and strength of the pinning potential.[16] In this paper we investigate the phenomenon of attenuation of low frequencies in random signal spectra for different values of the external magnetic field.

II. THEORETICAL MODEL

Let us consider a superconducting film composed of many grains linked by intrinsic Josephson junctions. The film is immersed in an external magnetic field, applied perpendicular to the film surface, and biased with a dc current flow. Abrikosov vortices created in the film by the self-field of the bias current and/or by the external magnetic field are pinned on natural pinning centers associated with film inhomogeneities. On the basis of experimental findings[17] we assume that in a Y-Ba-Cu-O thin film we deal with two different types of pinning centers: strong pinning centers which are trapping the major part of vortices and shallow ones. The shape of pinning potential depends on the space coordinate in the film and on the values of magnetic field and dc current flow. For current flow below the depinning current, Abrikosov vortices in the strong pinning centers undergo only small displacements from their equilibrium positions. Due to the action of the effective Lorentz force imposed by the bias current and magnetic screening current, the pinning potential will be stressed. For certain bias conditions, noisy window,[5-8] we may arrive to the situation in which two adjacent shallow pinning centers form a two-level fluctuator (TLF) consisting of two almost equal potential wells separated by an energy barrier and a flux line undergoing thermally activated jumps between the wells.[7,12,13] As it has been shown earlier, see the Introduction and references quoted therein, such jumps result in magnetic-flux random-telegraph signal. Flux noise may get converted into the voltage noise in the presence of Josephson dissipation in the film.[8] In our model we assume that random telegraph signal, generated by flux jumps, interacts with the remaining relatively strongly pinned Abrikosov vortices. Viscous relaxation of these vortices attenuates low frequencies of the random signal spectra. In order to account for this effect, in the following we will calculate a response of the system of strongly pinned vortices, in various experimental configurations, to the action of the external random force due to the flux jumps.

A. Basic equations

For a sample containing a number of vortices, the total voltage due to the vortex motion results from a superposition of contributions from individual vortices. The relation between voltage V_i produced by the ith vortex and the vortex velocity for a uniform thickness film is determined by the resolution function $\mathbf{g}(\boldsymbol{\rho}_i)$, where $\boldsymbol{\rho}_i$ is the ith vortex radius vector.[18] The form of this function depends on the geometry of the sample and on the voltage measuring circuit.

$$V_i=\mathbf{g}(\boldsymbol{\rho}_i)\cdot v_i \ , \qquad \mathbf{g}(\boldsymbol{\rho})=\frac{\phi_0}{4\pi I_m}[\mathbf{b}_{mt}(\boldsymbol{\rho})-\mathbf{b}_{mb}(\boldsymbol{\rho})] \ . \tag{1}$$

Here $\mathbf{v}_i$ is the vortex velocity, $\mathbf{b}_{mt}$ and $\mathbf{b}_{mb}$ are the values of $\mathbf{b}_m$ on the top and on the bottom of a slab, and $\mathbf{b}_m$ is the magnetic induction due to the current flow I_m in the measuring circuit. A vortex-flux density can be represented in the form[19]

$$\mathbf{J}(\boldsymbol{\rho},t)=\sum_i \mathbf{v}_i(t)\delta_2[\boldsymbol{\rho}-\boldsymbol{\rho}_i(t)] \ , \tag{2}$$

where t is the time. $\mathbf{J}(\rho,t)$ contains all information about the vortex dynamic. Total voltage due to the vortex motion is

$$V(t)=\int d^2\rho \mathbf{g}(\boldsymbol{\rho})\mathbf{J}(\boldsymbol{\rho},t) \ . \tag{3}$$

The noise component of the voltage $V(t)$ can be represented in the form

$$\delta V(t)=V(t)-\langle V(t)\rangle_t=\int d^2\rho \mathbf{g}(\boldsymbol{\rho})\delta\mathbf{J}(\boldsymbol{\rho},t) \ , \tag{4}$$

where $\delta\mathbf{J}(\boldsymbol{\rho},t)=\mathbf{J}(\boldsymbol{\rho},t)-\langle\mathbf{J}(\boldsymbol{\rho},t)\rangle_t$ and $\langle\cdots\rangle_t$ stands for the time average. The voltage autocorrelation function is

$$\Psi_v(\tau)=\langle\delta V(t)\delta V(t+\tau)\rangle_t = \int d^2\rho\int d^2\rho'\sum_{\alpha\beta} g_\alpha(\boldsymbol{\rho})g_\beta(\boldsymbol{\rho}')K_{\alpha\beta}(\boldsymbol{\rho},\boldsymbol{\rho}',\tau) \ , \tag{5}$$

where

$$K_{\alpha\beta}(\boldsymbol{\rho},\boldsymbol{\rho}',\tau)=\langle\delta J_\alpha(\boldsymbol{\rho},t)\delta J_\beta(\boldsymbol{\rho}',t+\tau)\rangle_t \tag{6}$$

is the vortex-flow correlation function, α and β are Cartesian coordinates. Observe that the voltage (3) and its autocorrelation function (5) depend both on the measuring circuit geometry and on the vortex dynamics. In the following we shall assume that function $K_{\alpha\beta}$ describing the

vortex dynamics is independent from the measuring circuit geometry.

Let us consider superconducting thin film containing rigid vortices. Positions of vortices in the slab are described by two-dimensional vectors ρ_i.[19] For a vortex with equilibrium position $\mathbf{a}_{i0}$ in the Abrikosov lattice frame (ALF) we write

$$\rho_i = \mathbf{a}_{i0} + \mathbf{u}(\mathbf{a}_{i0}, t) , \tag{7}$$

where $\mathbf{u}(\mathbf{a}_{i0}, t)$ is the deviation of a vortex from the point $\mathbf{a}_{i0}$.

The energy of interaction between vortices can be written in the harmonic approximation:

$$U(\mathbf{u}(\mathbf{a}_{i0}, t)) = \tfrac{1}{2} \sum_{ij} G(i,j)\mathbf{u}(\mathbf{a}_{i0}, t)\mathbf{u}(a_{j0}, t) , \tag{8}$$

where $G(i,j)$ is the elastic matrix. Vortex deviations $\mathbf{u}(\mathbf{a}_{i0}, t)$ can be expanded in the basis of polarization vectors $\varepsilon(\mathbf{q},\lambda)$ diagonalizing dynamic matrix $D(\mathbf{q};\lambda)$:

$$D(\mathbf{q})\varepsilon(\mathbf{q}\lambda) = D_{\mathbf{q}\lambda}\varepsilon(\mathbf{q}\lambda) , \tag{9}$$

where

$$D(\mathbf{q}) = \sum_{\mathbf{h}} G(\mathbf{h})\exp(i\mathbf{q}\mathbf{h}), \quad \mathbf{h} = \mathbf{a}_{i0} - \mathbf{a}_{j0} , \tag{10}$$

and

$$\mathbf{u}(\mathbf{a}_{i0}, t) = \sum_{\mathbf{q}\lambda} \varepsilon(\mathbf{q}\lambda)\exp(i\mathbf{q}\mathbf{a}_{i0}) Q_{\mathbf{q}\lambda} , \tag{11}$$

where $Q_{\mathbf{q}\lambda}(t)$ are the normal-mode amplitudes, $\mathbf{q}$ and λ are the wave vector and polarization, respectively.

According to Eq. (5) voltage noise can be expressed in the terms of vortex-flow correlation function. If the dimensions of the measuring circuit are large with respect to the intervortex spacing, we can treat the vortex lattice as a continuum. Within the first-order approximation, assuming small displacements of vortices from their equilibrium positions, the change in the vortex-flow density is

$$\delta\mathbf{J}(\rho, t) = n_0 \delta\mathbf{v}(\rho - \mathbf{v}_0 t, t) + \mathbf{v}_0 \delta n(\rho - \mathbf{v}_0 t, t) , \tag{12}$$

where n_0 is the equilibrium vortex density, $\delta\mathbf{J}$ and ρ are vectors in the laboratory reference frame, and $\delta\mathbf{v}$ and δn are measured in the ALF system moving with a velocity $\mathbf{v}_0$. Identifying $\delta\mathbf{v}$ as $d\mathbf{u}/dt$ and δn as $[-n_0 \nabla \mathbf{u}]$, we get from Eqs. (9)–(12)

$$\delta\mathbf{J}(\rho, t) = n_0 \sum_{\mathbf{q}\lambda} \left[\varepsilon(\mathbf{q}\lambda) \frac{dQ_{\mathbf{q}\lambda}}{dt} - i\mathbf{v}_0 \mathbf{q} \cdot \varepsilon(\mathbf{q}\lambda) Q_{\mathbf{q}\lambda}(t) \right] \times \exp[i\mathbf{q}(\rho - \mathbf{v}_0 t)] . \tag{13}$$

Putting $\delta\mathbf{J}$ from Eq. (13) into Eq. (4) we obtain for the noise voltage

$$\delta V(t) = \sum_{\mathbf{q}\lambda} \delta V_{\mathbf{q}\lambda}(t) , \tag{14}$$

with

$$\delta V_{\mathbf{q}\lambda}(t) = [F_{\mathbf{q}\lambda} dQ_{\mathbf{q}\lambda}(t)/dt + G_{\mathbf{q}\lambda} Q_{\mathbf{q}\lambda}(t)] \times \exp(-i\mathbf{q}\mathbf{v}_0 t) , \tag{15}$$

where

$$F_{\mathbf{q}\lambda} = n_0 \int d^2\rho \mathbf{g}(\rho)\varepsilon(\mathbf{q}\lambda)\exp(i\mathbf{q}\rho) . \tag{16}$$

and

$$G_{\mathbf{q}\lambda} = -n_0 \int d^2\rho \mathbf{g}(\rho)\mathbf{v}_0 \exp(i\mathbf{q}\rho)(i\mathbf{q}\varepsilon(\mathbf{q}\lambda)) . \tag{17}$$

Observe that there are two components in Eq. (15) describing the voltage noise. The first one is proportional to the velocity fluctuations, i.e., to $dQ_{\mathbf{q}\lambda}/dt$, while the second term is proportional to the vortex density fluctuations, i.e., to $Q_{\mathbf{q}\lambda}$. Let us consider two different configurations of the sample and voltage measuring circuit.

1. *Infinite film with parallel vertical voltage measuring leads*

The considered geometry is illustrated in Fig. 1(a). Thin infinitely long parallel vertical leads are attached to the superconductor at the points a and b. In this case we rewrite Eq. (1) as[18]

$$\mathbf{g}(\rho) = -\frac{\phi_0}{4\pi} [\mathbf{b}_{m_a}(\rho) + \mathbf{b}_{m_b}(\rho)] , \tag{18}$$

where ρ is the vortex position on the top of the slab. Assuming that $|\rho - \rho_{a;b}|$ is larger than the voltage lead radius R one can write for $\mathbf{b}_m(\rho)$

$$\mathbf{b}_{m_{a;b}}(\rho) = \pm 2 \frac{\mathbf{n} \times (\rho - \rho_{a;b})}{c|\rho - \rho_{a;b}|^2} , \tag{19}$$

where $\mathbf{n} = \mathbf{B}/|\mathbf{B}|$ is the unitary vector of magnetic induction in the film. Putting Eq. (18) into (16) and (17) we ob-

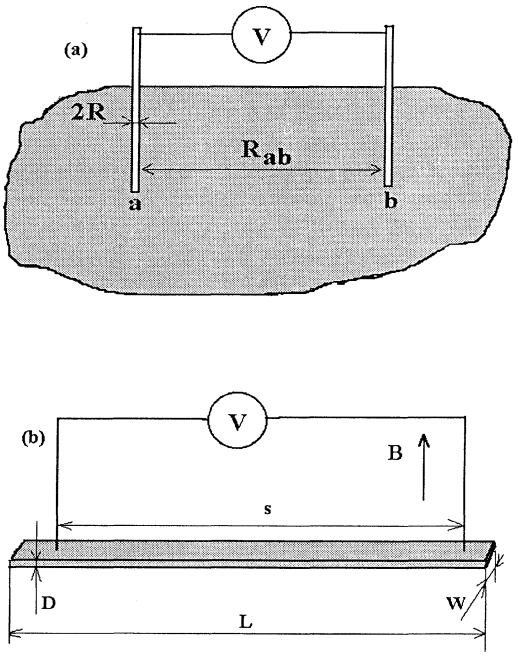

FIG. 1. Geometry of the considered problem: (a) finite film, and (b) thin-film strip.

tain the following expressions for $F_{q\lambda}$ and $G_{q\lambda}$:

$$F_{q\lambda}=\mathbf{B}[\varepsilon(q\lambda)\times\frac{\mathbf{q}}{|\mathbf{q}|}[\exp(i\mathbf{q}\rho_a)-\exp(i\mathbf{q}\rho_b)]\times\frac{J_0(qR)\delta_{\lambda;\mathrm{tr}}}{i|\mathbf{q}|c}\ , \tag{20}$$

$$G_{q\lambda}=\mathbf{B}\left[\frac{q}{|q|}\times v_0\right][\exp(i\mathbf{q}\rho_a)-\exp(i\mathbf{q}\rho_b)]\times\frac{J_0(qR)\delta_{\lambda;\mathrm{lo}}}{c}\ , \tag{21}$$

where J_0 is the Bessel function of the first kind, $\delta_{\lambda;\mathrm{tr}}$ and $\delta_{\lambda;\mathrm{lo}}$ are the Kroneckers symbols for the transverse and longitudinal polarizations, respectively.

2. *Infinite strip with voltage measuring leads far away from the surface*

For a strip possessing length L in the x direction, width W in the y direction, and thickness D in the z direction, such that $L\gg W\gg D$ and having measuring leads attached at points $[x_a,0]$ and $[x_b,0]$ such that $x_a-x_b=s\gg W$, see Fig. 1(b), the resolution function $\mathbf{g}(\rho)$ is[20]

$$\mathbf{g}(\rho)=\frac{\phi_0}{2\pi c}\left[\left[\frac{W}{2}\right]^2-y^2\right]^{-1/2}\mathbf{e}_y\ , \tag{22}$$

where $\mathbf{e}_y$ is the unit vector in the y direction. Equation (22) holds for vortices moving between the leads far away from the contacts. A more complicated expression would arise if a vortex position would fall within a distance less than W from the contacts. Nevertheless, the condition $s\gg W$ allows us to neglect contributions of such vortices. Proceeding as in the previous case we obtain for $F_{q\lambda}$ and $G_{q\lambda}$

$$F_{q\lambda}=\frac{|\mathbf{B}|s}{2c}J_0\left[\frac{q_yW}{2}\right]\delta_{q_x;0}\delta_{\lambda;\mathrm{lo}}\ , \tag{23}$$

$$G_{q\lambda}=\frac{|\mathbf{B}|s}{2c}(\mathbf{q}\cdot\mathbf{v}_0)J_0\left[\frac{q_yW}{2}\right]\delta_{q_x;0}\delta_{\lambda;\mathrm{lo}}\ . \tag{24}$$

3. *Vortex motion*

The phenomenological equation of force balance for a moving ith vortex is

$$\eta\frac{d\rho_i}{dt}=-\sum_j G(j,i)\mathbf{u}(j,t)+\mathbf{f}_{\mathrm{ext}}(\rho_i,t)\ , \tag{25}$$

where η is the vortex viscosity per unit length, $\mathbf{f}_{\mathrm{ext}}(\rho_i,t)$ is the linear density of the external force, while the vortex-vortex interaction term is accounted for according to Eq. (8). Taking the time average of Eq. (25), we obtain for vortices displacements from equilibrium positions

$$\eta\frac{d\mathbf{u}(\mathbf{a}_{i0},t)}{dt}+\sum_j G(i,j)\mathbf{u}(\mathbf{a}_{j0},t)=\delta\mathbf{f}(\mathbf{a}_{i0},t)\ , \tag{26}$$

where $\delta\mathbf{f}=\mathbf{f}_{\mathrm{ext}}-\langle\mathbf{f}\rangle$. Expanding Eq. (26) by the normal displacements, we obtain

$$\eta\frac{dQ\mathbf{q}\lambda(t)}{dt}+D_{q\lambda}Q_{q\lambda}(t)=\delta f_{q\lambda}(t)\ , \tag{27}$$

where

$$\delta f_{q\lambda}=\frac{1}{N}\sum_j\exp(-i\mathbf{q}\mathbf{a}_{j0})\varepsilon(\mathbf{q}\lambda)\delta\mathbf{f}(\mathbf{a}_{j0},t)\ , \tag{28}$$

and N is the number of vortices. The solution of Eq. (27) is

$$Q_{q\lambda}=\int_{-\infty}^{\infty}\frac{d\omega}{2\pi}\sigma_\lambda(\mathbf{q},\omega)\delta f_{q\lambda}(\omega)\exp(-i\omega t)\ , \tag{29}$$

$$\sigma_\lambda(\mathbf{q},\omega)=-[i\omega\eta-\mathbf{D}_{q\lambda}]^{-1}\ . \tag{30}$$

Knowing the fluctuating component of the external force, $\delta\mathbf{f}$, we can calculate $Q_{q\lambda}$ and $dQ_{q\lambda}/dt$, and thus the resulting noise voltage.

B. Random-telegraph noise in granular film

According to the assumptions of our model we divide the system of vortices into two subsystems. Weakly pinned vortices generate random-telegraph signals at appropriate bias conditions, while strongly pinned ones behave differently in different experimental situations. We account for the telegraph signal by introducing an external force into Eq. (25) in the form of a random force providing a random-telegraph correlation function in the time domain.

1. *Dense Abrikosov lattice in grains*

In the following we shall consider a thin granular superconducting film with an average grain size d. The Abrikosov vortex lattice is created in each grain by a sufficiently strong magnetic field applied perpendicular to the film surface. Let us assume the presence of RTN voltage in the sample. RTN voltage results in additional random currents flowing along the grains and consequently in a random Lorentz force acting on Abrikosov vortex lattice inside the grains. Observe that the Lorentz force due to RTN is a random function depending both on time and on space coordinates. Spatial dependence is due to the inhomogeneity of the considered system, in particular to the distribution of magnetic induction in the grains and to the spatial distribution of current density. One can separate time and coordinate dependent components of the force-force correlators, assuming that they are independent. The spatially dependent factor can be written, for the simplicity sake, in the exponential form. Time randomness of the signal is included in the time-dependent part of the correlator $Z(t,t')$

$$Z(\rho,\rho',t,t')=\langle\delta\mathbf{f}(\rho,t)\delta\mathbf{f}(\rho',t')\rangle=Z(t,t')\exp(-\mathbf{q}_l|\rho-\rho'|)\ . \tag{31}$$

The quantity $\mathbf{q}_l$ is determined by $[1/l,1/l]$, where l is the correlation length. It is reasonable to assume that in a granular sample l will be of the order of the characteristic size of the grains. For RTN-induced random force one should write $Z(t,t')$ in the form

$$Z(t,t')=Z_0\exp\left[\frac{|t-t'|}{\tau}\right], \tag{32}$$

where Z_0 is the mean square of the Lorentz force fluctuations.

Spectral density of fluctuations, using Eqs. (5) and (15)–(17), can be represented in the form

$$P_v(\omega)=\sum_{q\lambda}[F_{q\lambda}^2\omega'^2+2iF_{q\lambda}G_{q\lambda}\omega'-G_{q\lambda}^2]\times Z(\mathbf{q},\omega')|\sigma(\mathbf{q},\omega')|^2, \tag{33}$$

$$Z(\mathbf{q},\omega)=\frac{1}{S}\int Z(\mathbf{r},t)\exp(i\omega t+i\mathbf{qr})d^2\mathbf{r}dt, \tag{34}$$

where $\omega'=\omega-\mathbf{qv}_0$ and S is the surface of the sample.

Assuming that all Abrikosov vortices are pinned inside the grains, $\mathbf{v}_0=0$, we obtain from (21) and (24) that $G_{q\lambda}=0$. Performing a Fourier transform of (31) and (32) and putting them into (33), one can obtain an expression for $P_v(\omega)$ due to the action of an external RTN. Now, as in Sec. II A, we shall consider two different types of measuring circuit.

a. Infinite film with parallel vertical leads. For this configuration of the measuring circuit we derive from Eq. (33) using Eq. (20)

$$P_v(\omega)=\frac{4C}{l^2}\frac{\omega^2}{(\omega\tau)^2+1}\int q\,dq\int d\varphi\frac{\sin^2(\mathbf{q}\cdot\mathbf{R}_{ab}/2)J_0^2(qR)q_0^2\cos^2\varphi}{q^2[q^2\cos^2\varphi+q_0^2][q^2\sin^2\varphi+q_0^2][D_{qtr}^2+(\eta\omega)^2]},$$
$$D_{qtr}=\phi_0q^2C_{66}/B,\quad C=\frac{Z_0\tau B^2l^2}{c^2}, \tag{35}$$

where $q_0=1/l$, φ is the angle between $\mathbf{q}$ and $\mathbf{v}_0$ (x axis). C_{66} is the shear modulus of Abrikosov lattice, and B stands for $|\mathbf{B}|$. The integration in (35) is performed over the first Brillouin zone of the reciprocal lattice of Abrikosov vortices. For sufficiently dense lattice the shear modulus is[21]

$$C_{66}=\phi_0B/(8\pi\lambda)^2; \tag{36}$$

therefore, the magnitude of spectral density depends on magnetic field as $P_v(\omega)\propto B^2$.

Let us have a closer look at the spectral density function at various frequency ranges:

(i) For extremely small frequencies, $\omega\ll\omega_r$, where characteristic frequency $\omega_r=\phi_0C_{66}/B\eta R_{ab}^2$, one gets from the integral (35)

$$P_v(\omega)=\frac{3\pi^2}{16\eta^2}\frac{C}{[(\omega\tau)^2+1]}\frac{\omega}{\omega_r}. \tag{37}$$

Observe that at low frequencies power spectrum (35) decreases linearly with decreasing frequency and approaches zero when frequency $\omega\to0$.

(ii) For intermediate frequencies, $\omega_r\ll\omega\ll\omega_c$, where the characteristic frequency $\omega_c=\phi_0C_{66}/B\eta l^2$, we obtain an asymptotic result valid for $l\gg R$,

$$P_V(\omega)=\frac{\pi}{4\eta^2}\frac{C}{[(\omega\tau)^2+1]}\ln\left[\frac{\omega}{\omega_r}\right]. \tag{38}$$

(iii) For large frequencies, $\omega\gg\omega_c$, the vortex lattice cannot damp the random-telegraph signal because the integral (35) does not depend on the shear modulus at all. As a result we get, assuming again that $l\gg R$,

$$P_v(\omega)=\frac{4}{l^2\eta^2}\frac{C}{[(\omega\tau)^2+1]}I_f(q_0);$$
$$I_f(q_0)=\int q\,dq\int d\varphi\frac{\sin^2(\mathbf{q}\cdot\mathbf{R}_{ab}/2)J_0^2(qR)q_0^2\cos^2\varphi}{q^2[q^2\cos^2\varphi+q_0^2][q^2\sin^2\varphi+q_0^2]}. \tag{39}$$

For the opposite case of large diameter voltage leads, $R\gg l$, the formulas remain valid if the characteristic frequency ω_c will be substituted by $\omega_R=\phi_0C_{66}/B\eta R^2$.

The overall shape of power spectrum for a dense Abrikosov lattice interacting with a random-telegraph signal in an infinite film is schematically presented in Fig. 2(a).

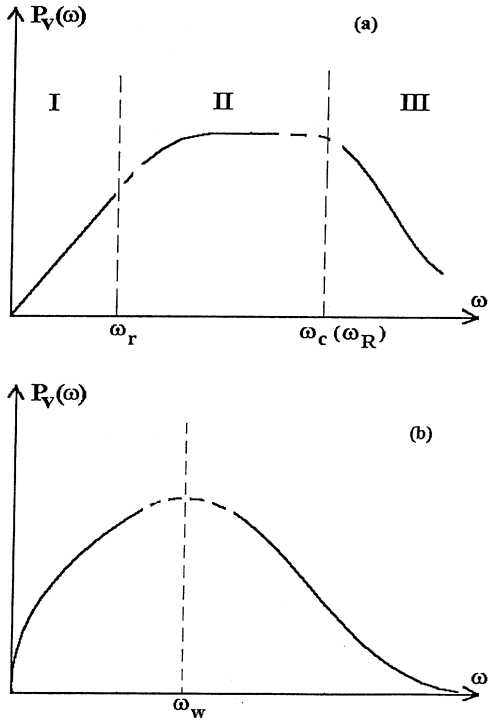

FIG. 2. Qualitative behavior of power spectrum for an infinite film geometry (a), and for an infinite thin-film strip (b) for high magnetic fields (dense Abrikosov lattice) and for medium magnetic fields (soft, low density lattice).

Note the appearance of the maximum in the spectrum at a frequency of the order of ω_c (ω_R). Since the shear modulus of Abrikosov vortex lattice is proportional to B, see Eq. (36), all characteristic frequencies do not depend on magnetic field. Evidently, the shape of $P_v(\omega)$ depends on the relation between the correlation length l and parameters of the measuring system R_{ab} and R, i.e., eventually on the sample microstructure.

b. Infinite strip, leads kept far from the surface. For the infinite strip with leads placed far away from the surface we derive from Eq. (33) using Eq. (23),

$$P_v(\omega)=\frac{Cs^2}{4l^2}\frac{\omega^2}{(\omega\tau)^2+1}\int dq\frac{J_0^2(qW/2)q_0}{[D_{ql0}^2+\eta^2\omega^2][q^2+q_0^2]}\ , \tag{40}$$

$$D_{ql0}=\phi_0 q^2 C_{11}/B,\ \text{ and } C=\frac{Z_0\tau B^2 l^2}{c^2}\ .$$

Observe that in this case, according to Eq. (23), random external signal interacts with longitudinal displacements of Abrikosov lattice only. Elastic constant corresponding to these displacements is proportional to the bulk compressive modulus of the Abrikosov lattice C_{11}.[16] Therefore, we have only one characteristic frequency ω_w which depends on the strip width $\omega_w=\phi_0 C_{11}/B\eta w^2$. For limiting frequency ranges we have:

(i) At extremely small frequencies $\omega\ll\omega_w$,

$$P_v(\omega)=\frac{Cs^2}{8\eta^2 lW}\frac{(2\omega/\omega_w)^{1/2}}{[(\omega\tau)^2+1]}, \tag{41}$$

the power spectrum goes to zero with decreasing frequency as $\omega^{1/2}$. For sufficiently strong magnetic fields the modulus C_{11}, in a long-wave limit, can be expressed as $C_{11}=B^2/4\pi$.[16] The characteristic frequency ω_w becomes thus field dependent, $\omega_w=\phi_0 B/4\pi\eta W^2$, while the spectrum magnitude $P_v(\omega)\propto B^{3/2}$.

(ii) For large frequencies $\omega\gg\omega_w$ we find

$$P_v(\omega)=\frac{s^2}{4l^2\eta^2}\frac{C}{[(\omega\tau)^2+1]}I_s(q_0)\ ,$$
$$I_s(q_0)=\int dq\frac{q_0}{(q^2+q_0^2)}J_0^2(qW/2)\ , \tag{42}$$

and the power spectrum is undisturbed by the vortex system. The magnitude of the power spectrum is simply proportional to B^2. The schematic shape of the power spectrum for an infinite strip is shown in Fig. 2(b). In a marked difference to the infinite film case, the broad maximum is substituted now by a peak centered at a characteristic frequency ω_w.

Let us underline that due to a finite width of the strip the effect of suppression of the low-frequency part of power spectra will exist even for a uniform distribution of the current flow density in the strip. In this case only the time-dependent part of Eq. (31) is important. Evaluating the integral in Eq. (34) we obtain for $P_v(\omega)$

$$P_v(\omega)=\frac{C}{4W}\left[\frac{s}{l}\right]^2\frac{\omega^2}{(\omega\tau)^2+1}\times\int dq\frac{\sin^2(qW/2)J_0^2(qW/2)}{(D_{ql0}^2+\eta^2\omega^2)q^2}\ . \tag{43}$$

For small and large frequency range we get, respectively,

$$P_v(\omega)=\frac{Z_0\tau s^2 B^{5/2}W}{16(2\phi_0 C_{11})^{1/2}\eta^{3/2}c^2}\frac{\omega^{1/2}}{[(\omega\tau)^2+1]},\quad \omega\ll\omega_w;$$
$$P_v(\omega)\propto\frac{s^2}{4\eta^2}\frac{1}{[(\omega\tau)^2+1]},\quad \omega\gg\omega_w\ . \tag{44}$$

At low frequencies the dependence $P_v(\omega)$ is identical to that given by Eq. (41), assuming that the correlation length $l=1/q_0$ extends to the entire width of the strip W. At high frequencies we observe an unperturbed Lorentzian shape with a geometry-dependent magnitude.

2. *Low density Abrikosov lattice in grains*

If the intervortex distance $d_0=(\phi_0/B)^{1/2}$ exceeds the magnetic penetration length λ the vortex lattice becomes smoother, the elastic modulus C_{66} changes dramatically and becomes[22]

$$3C_{66}=C_{11}=(3\pi/2)^{1/2}\varepsilon_0/\lambda^2(\lambda/d_0)^{1/2}\exp(-d_0/\lambda)\ , \tag{45}$$

where ε_0 is the vortex energy. Putting (45) into Eqs. (37), (38), and (41) we find that the power spectrum $P_v(\omega)$ depends on the magnetic field in a nontrivial way. For particular setups we have:

(a) Infinite film with parallel vertical leads.

(i) Extremely small frequencies $\omega\ll\omega_r$;

$$P_v(\omega)=\alpha B^{11/4}\exp(\beta B^{-1/2})\ , \tag{46}$$

where

$$\alpha=\frac{3Z_0\tau l^2\pi^2 R_{ab}^2\lambda^2}{16\eta\phi_0 c^2\varepsilon_0(\pi/6\beta)^{1/2}}\frac{\omega}{[(\omega\tau)^2+1]}$$

and

$$\beta=\sqrt{\phi_0/\lambda^2}\ .$$

(ii) Intermediate frequencies $\omega_r\ll\omega\ll\omega_c$, ($\omega_R$);

$$P_v(\omega)=\alpha_1 B^2(\alpha_2+\tfrac{3}{4}\ln B+\beta B^{-1/2})\ , \tag{47}$$

where

$$\alpha_1=\frac{Z_0\tau l^2\pi}{4c^2\eta^2[(\omega\tau)^2+1]},\quad \alpha_2=\ln\left[\frac{\omega\eta\lambda^2R_{ab}^2}{\varepsilon_0\phi_0(\pi/6\beta)^{1/2}}\right]\ .$$

(iii) Very high frequencies $\omega\gg\omega_c(\omega_R)$; At high frequencies, as was in the case of a dense Abrikosov lattice, the power spectrum does not depend on C_{66} and $P_v(\omega)\propto B^2$.

Note that in a marked difference to a dense lattice for a soft Abrikosov lattice in an infinite film the characteristic frequencies are magnetic-field dependent. Indeed, taking

into account (45) we have

$$\omega_r=\frac{\phi_0 C_{66}}{B\eta R_{ab}^2}=\frac{(\pi/6)^{1/2}\varepsilon_0 d_0^{3/2}\exp(-d_0/\lambda)}{\eta\lambda^{3/2}R_{ab}^2} . \quad (48)$$

The frequencies ω_c and ω_R depend on B in an analogous way.

(b) Infinite strip with leads kept far away from the surface. For extremely small frequencies below a characteristic frequency ω_w,

$$\omega_w=\frac{\phi_0 C_{11}}{B\eta W^2}=\frac{(3\pi/2)^{1/2}\varepsilon_0 d_0^{3/2}\exp(-d_0/\lambda)}{\eta\lambda^{3/2}W^2} , \quad (49)$$

the power spectrum takes the form

$$P_v(\omega)=\gamma B^{19/8}\exp\left[\frac{\beta B^{-1/2}}{2}\right] , \quad (50)$$

where

$$\gamma=\frac{Z_0\tau\lambda^2 s^2}{4q_0(3\pi\phi_0/2\beta)^{1/4}\varepsilon_0^{1/2}\eta^{3/2}c^2}\frac{\omega^{1/2}}{[(\omega\tau)^2+1]} . \quad (51)$$

For frequencies $\omega\gg\omega_w$, as in all previous cases, $P_v(\omega)\propto B^2$.

3. *Single vortex in the pinning center*

In small magnetic fields the vortex interaction with individual pinning centers becomes significant. In this case we can neglect, in the first order, the vortex-vortex interaction and take into account only the vortex motion in an individual pinning center. The equation of motion of a single vortex with equilibrium state coordinate ρ_0 takes a simple form, see Eq. (26),

$$\eta d\mathbf{u}_i(\rho_0)/dt+K\mathbf{u}_i(\rho_0)=\delta\mathbf{f}(\rho_0) . \quad (52)$$

In Eq. (52), $\delta\mathbf{f}$ and $\mathbf{u}$ are directed along the y axis, $K=(d^2U/dy^2)$, and $U(\rho_0)$ is vortex potential energy in a pinning center. Observe that the suppression of the power spectrum by single pinned vortices will exist also for spatial coherence extending into the entire sample, $l\to\infty$, see Eq. (31). Indeed, it follows from Eq. (33), leaving in the sum only the term with $k=0$, that power spectrum is

$$P_v(\omega)=\frac{Z_0B^2\tau}{\phi_0^2\eta^2}\left[\int\mathbf{g}(\rho)d^2\rho\right]^2\frac{\omega^2}{[(\omega\tau)^2+1][\omega_p^2+\omega^2]} , \quad (53)$$

where $\omega_p=K/\eta$ is the characteristic pinning frequency. Note that in the case of single vortices enclosed in the grains this frequency may be set by the surface barriers of the grain boundaries (surface pinning). For the strip geometry we take $\mathbf{g}(\rho)$ from Eq. (22) and obtain

$$P_v(\omega)=\frac{B^2s^2Z_0\tau}{4c^2\eta^2}\frac{\omega^2}{[(\omega\tau)^2+1][\omega_p^2+\omega^2]} . \quad (54)$$

$P_v(\omega)$ calculated according to Eq. (54) is presented in Fig. 3. In a marked difference to the previously discussed cases of Abrikosov lattices, with decreasing frequency the power spectrum goes to zero as ω^2. Due to vortex relaxation the spectrum has a maximum at a frequency

$$\omega_0=(\omega_p/\tau)^{1/2} , \quad (55)$$

and behaves as a Lorentzian at frequencies $\omega\gg\omega_p$.

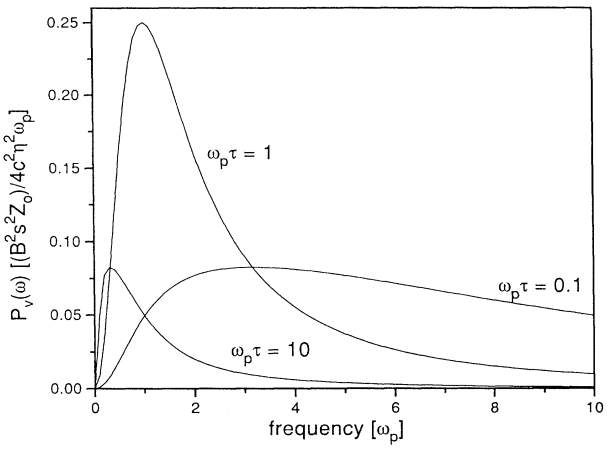

FIG. 3. Power spectrum in the case of thin-film strip immersed in low magnetic field (single vortices in grains). Different spectra are plotted for different value of RTN cutoff frequencies measured in $\omega_p\tau$ units. Note that the frequencies measured in $\omega_p\tau$ units. Note that the frequency is measured in the units of ω_p.

III. CONCLUSION

In conclusion, we have theoretically predicted the effect of suppression of the low-frequency part of the power spectra of random-telegraph signals in various superconducting systems. In particular, we have shown that the effect will be most pronounced in the granular films where the suppression of the spectra is due to the vortex-vortex interactions. According to the model, roll-on frequency of the RTN spectra for a superconductor containing a pinned Abrikosov lattice depends on the characteristic frequency of the vortex system, namely on the lattice elastic matrix, vortex viscosity, and the characteristic length of the measuring circuit. This length corresponds to the distance between the contacts, in the case of an infinite film, and to the width of the film in the case of a long strip.

The suppression effect should be easily observed experimentally for RTN signals with sufficiently high switching rates like those observed by us in granular YBCO thin films.[8] Let us estimate the roll-on frequency ω_{on} below which the RTN power spectrum will be suppressed. We shall consider a typical experimental configuration of an Abrikosov lattice in a long narrow strip, strip width of the order $W\sim10^{-2}$ cm, and of single pinned vortices in a granular strip. For the case of Abrikosov lattice the roll-on frequency corresponds to $\omega_w=\phi_0C_{11}/B\eta W^2$, see (41) and (42). Assuming that vortex viscosity in the strip is of the order $\eta\sim10^{-7}$ g/cm s,[23] and putting for the bulk compressive modulus in low

TABLE I. Estimation of the roll-on frequency below which RTN power spectra might get suppressed due to the relaxation of pinned vortices in a narrow (0.01 cm width) thin-film strip.

Configuration: magnetic field:	Abrikosov lattice strong field $B \sim 10^3$ Gs	Abrikosov lattice low field $B \sim 50$ Gs	Single vortices very low field
ω_{on}	10^6 Hz	10^4 Hz	$10^9 - 10^{11}$ Hz

magnetic fields Eq. (45), while in strong fields approximating it by $C_{11} = B^2/4\pi$,[16] we obtain the results shown in Table I. For the case of single pinned vortices the roll-on frequency ω_{on} corresponds to the pinning frequency $\omega_p = K/\eta$. Values quoted for ω_p in Table I are taken from the recent experimental evaluations.[23] Let us underline that in the case of vortices pinned inside the grains by means of the surface pinning the equivalent pinning frequency, set by the size of the grain, may be of orders of magnitude lower.

In real experimental situations the macroscopic RTN signals are usually accompanied by the background fluctuations frequently taking a form of $1/f$ noise. The $1/f$ noise influences the shape of power spectra and in particular changes the values of characteristic frequencies, thus changes the position of the maximum. This problem will be discussed by us elsewhere.

Although the present paper deals with RTN spectra we would like to underline that the described effect of suppression should be observed for an arbitrary external signal, random or deterministic, applied to the superconducting system. The physical mechanism of the suppression is generally associated with the action of the pinned vortex system opposing the external force. In fact, there are experimental data in the literature clearly demonstrating spectra with suppressed low-frequency parts.[24-29] Nevertheless, most of the hitherto reported spectra are free from the low-frequency suppression effect. According to the presented model the suppression should not be observed in infinite nongranular films at low magnetic fields at which vortex-vortex interactions can be neglected. The latter case has been investigated by some of us in a recent experiment performed with an epitaxial BSCCO film at 77 K and indeed, no anomalies were detected in the RTN voltage power spectra.[6] The effect should also vanish for flux-flow dissipation at high velocities of flowing vortices. We are currently investigating this problem.

In the present paper we have restricted ourselves to the investigation of pinned vortex systems with mean velocity equal to zero. It is easy to imagine that the effect should not vanish abruptly when vortices start to flow with sufficiently low velocities, as is probably the case of several spectra reported in Refs. 27 and 28.

ACKNOWLEDGMENTS

This work was partially supported by the KBN Grant No. 2 P302 179 06. We also thank the Ministry of Science and Arts of Israel, Israel Academy of Sciences, and Rashi foundation for their support.

[1]M. J. Ferrari, Mark Johnson, F. C. Wellstood, J. J. Kingston, T. J. Shaw, and John Clarke, J. Low Temp. Phys. **94**, 15 (1994), and references quoted therein.
[2]L. B. Kiss and P. Svendingh, IEEE Trans. Electron Devices (to be published) and references therein.
[3]C. T. Rogers, K. E. Myers, J. N. Eckstein, and I. Bozovic, Phys. Rev. Lett. **69**, 160 (1992).
[4]M. J. Ferrari, F. C. Wellstood, J. J. Kingston, and John Clarke, Phys. Rev. Lett. **67**, 1346 (1991).
[5]M. Bonaldi, G. Jung, B. Savo, A. Vecchione, and S. Vitale, Physica B **194-196**, 2037 (1994).
[6]P. Gierlowski, G. Jung, W. Kula, S. J. Lewandowski, B. Savo, R. Sobolewski, A. Tebbiano, and A. Vecchione, Physica B **194-196**, 2043 (1994).
[7]G. Jung, B. Savo, and A. Vecchione, Europhys. Lett. **21**, 947 (1993).
[8]G. Jung, S. Vitale, J. Konopka, and M. Bonaldi, J. Appl. Phys. **70**, 5440 (1991).
[9]P. Dutta and P. M. Horn, Rev. Mod. Phys. **53**, 497 (1981).
[10]M. B. Weissman, Rev. Mod. Phys. **60**, 537 (1988).
[11]Sh. M. Kogan, Usp. Fiz. Nauk **145**, 285 (1985) [Sov. Phys. Usp. **28**, 170 (1985)].
[12]M. J. Kurton and M. J. Uren, Adv. Phys. **38**, 367 (1989).
[13]R. Kree and S. Thesis, Rev. Solid State Sci. **3**, 115 (1989).
[14]S. J. Lewandowski, Phys. Rev. B **43**, 7776 (1991); **45**, 2319 (1992).
[15]M. Darula, P. Seidel, F. Busse, and B. Beniacka, J. Appl. Phys. **74**, 2674 (1993).
[16]G. Blatter, M. V. Feigelman, V. B. Geshkenbein, A. I. Larkin, and V. M. Vinokur, Rev. Mod. Phys. (to be published).
[17]N.-C. Yeh, Phys. Rev. B **40**, 4566 (1989); V. N. Zavaritskii and N. V. Zavaritskii, Pis'ma Zh. Eksp. Teor. Fiz. **54**, 335 (1991) [JETP Lett. **54**, 330 (1991)].
[18]J. R. Clem, J. Phys. (Paris) **39**, C6-619 (1978).
[19]P. S. Li and J. R. Clem, Phys. Rev. B **23**, 2209 (1981).
[20]J. R. Clem, Phys. Rep. **75**, 1 (1981).
[21]E. H. Brandt, J. Low Temp. Phys. **26**, 735 (1977).
[22]A. I. Larkin, Zh. Eksp. Teor. Fiz. **58**, 1466 (1970) [Sov. Phys. JETP **31**, 784 (1970)].
[23]M. Golosovsky, M. Tsindlekht, H. Chayet, and D. Davidov, Phys. Rev. B **50**, 470 (1994).
[24]K. H. Han, M. K. Joo, Sung-Ho Suck Salk, H. J. Shin, and Sung-Ik Lee, Phys. Rev. B **46**, 11 835 (1992).
[25]A. Maeda, Y. Nakayama, S. Takebayashi, and K. Uchi-

nokura, Physica C **160**, 443 (1989).
[26]A. Hirai, T. Hotta, K. Shinoda, M. Sato, S. Sasaki, K. Iijima, K. Yamamoto, K. Hayashi, K. Hirata, T. Terashima, and Y. Bando, Cryogenics **30**, 910 (1990).
[27]D. J. van Oojen and G. J. van Garp, Phys. Lett. **17**, 230 (1965).
[28]D. J. van Oojen and G. J. van Garp, Phillips Res. Rep. **20**, 505 (1966).
[29]B. Placais and Y. Simon, Phys. Rev. B **39**, 2151 (1989).